Single Particle Dynamics at the Free Surface of Imidazolium-Based Ionic Liquids

Helga Tóth Ugyonka,[1] György Hantal,[2] István Szilágyi,[3] Abdenacer Idrissi,[4] Miguel Jorge,[5] and Pál Jedlovszky[1*]

[1]*Department of Chemistry, Eszterházy Károly Catholic University, Leányka utca 12, H-3300 Eger, Hungary*

[2]*PULS Group, Department of Physics, Friedrich-Alexander-Universität Erlangen-Nürnberg, Cauerstr. 3, D-91058 Erlangen, Germany*

[3]*MTA-SZTE Lendület Biocolloids Research Group, Department of Physical Chemistry and Materials Science, Interdisciplinary Excellence Center, University of Szeged, H-6720 Szeged, Hungary*

[4]*University of Lille, CNRS UMR 8516 -LASIRe - Laboratoire Avancé de Spectroscopie pour les Interactions la Réactivité et l'environnement, 59000 Lille, France*

[5]*Department of Chemical and Process Engineering, University of Strathclyde, 75 Montrose Street, Glasgow G1 1XJ, United Kingdom*

e-mail: jedlovszky.pal@uni-eszterhazy.hu (P.J.)

Abstract:

In this work, we carry out a systematic computer simulation investigation of the single particle dynamics at the free surface of imidazolium-based room temperature ionic liquids (RTILs) by applying intrinsic surface analysis. Besides assessing the effect of the potential model and temperature, we focus in particular on the effect of changing the anion type, and, hence, their shape and size. Further, we also address the role of the length of the cation alkyl chains, known to protrude into the vapor phase, on the surface dynamics of the ions. We observe that the surface dynamics of ionic liquids, being dominated by strong electrostatic interactions, are about two orders of magnitude slower than that for common molecular liquids. Furthermore, the free energy driving force for exposing apolar chains to the vapor phase "pins" the cations at the surface layer for much longer than anions, allowing them to perform noticeable lateral diffusion at the liquid surface during their stay there. On the other hand, anions, accumulated in the second layer beneath the liquid surface, stay considerably longer here than in the surface layer. The ratio of the mean surface residence time of the cations and anions depends on the relative size of the two ions: larger size asymmetry typically corresponds to larger values of this ratio. We also find, in a clear contrast with the bulk liquid phase behavior, that anions typically diffuse faster at the liquid surface than cations. Finally, our results show that the surface dynamics of the ions is largely determined by the apolar layer of the cation alkyl chains at the liquid surface, as in the absence of such a layer, cations and anions are found to behave similarly with respect to their single particle dynamics.

1. Introduction

Liquid phase salts at ambient conditions, often referred to as room temperature ionic liquids (RTILs), emerged as a new class of solvents more than two decades ago.[1] Compared to the traditional organic solvents, many RTILs possess a number of attractive physico-chemical properties, such as low volatility, negligibly small vapor pressure, broad electrochemical window, large thermal stability, as well as good miscibility and solvation properties. Due to their extremely low vapor pressure and, hence, negligible atmospheric pollution, RTILs are often claimed to be 'green' solvents, although their high persistence in aquatic and terrestrial environments, posing significant risks to ecosystems and human health cannot be neglected.[2-4] Moreover, the large variety of the possible cations and anions allows one to tune these properties systematically according to the specific requirements of the task to be done.[5] The above attractive features of RTILs originate from the fact that first order chemical interaction (i.e., ionic bond) acts between the oppositely charged ions; yet, the system is in the liquid phase under ambient conditions. The unusually low melting point of these systems is caused by the large asymmetry of the size, shape, and chemical character of the cations and anions. Thus, the properties of these systems are determined by a delicate interplay of the charge-charge, steric, H-bonding and hydrophobic interactions acting either between these ions or between some of their moieties. These peculiar features enable RTILs to be used as solvents in a variety of fields in chemistry and chemical engineering. Their potential applications range from electrochemistry[6] to gas capture,[7-9] from heat transfer[10] to chemical synthesis,[5] and from energy storage and conversion[10] to particle dispersant.[11,12] Further, the addition of certain specific groups to either of the ions can endow RTILs with, e.g., thermochromic, luminescent, or magnetoresponsive features.[13]

Since many of these applications involve also the surface of the RTIL, besides their bulk properties,[14-27] the interface of RTILs formed with other phases has also been the subject of intensive scientific investigations in the past decades, both by experimental[28-33] and computer simulation methods.[33-53] In this context, it is important to emphasize that when a fluid interface, such as the free surface of a RTIL, is seen at atomistic resolution, the surface is corrugated by capillary waves,[54] the smearing effect of which has thus to be removed in any meaningful analysis. Following the pioneering work of Chacón and Tarazona in 2003,[55] a number of methods capable of fulfilling this task and finding the real, capillary wave corrugated, so-called "intrinsic" surface of the liquid phase have been proposed.[56-61] Among these methods, the **i**dentification of the **t**ruly **i**nterfacial **m**olecules (ITIM)[58] represents an

optimal balance between computational cost and accuracy.[60] It has also been demonstrated several times that the neglect of the smearing effect of the capillary waves introduces a systematic error of unknown magnitude in the calculated properties of the interface,[58,62-64] which even propagates to the determination of the thermodynamic properties of the system.[65] In the wake of these realizations, the structure of the intrinsic surface of various RTILs has been the subject of an increasing number of computer simulation investigations in the past decade.[44-46,48,51-53,66,67]

Despite the wealth of such studies, relatively little attention has been paid to the dynamics of the ions at the liquid surface both in experiments[68] and computer simulations,[45,48,66,67,69-71] although this factor can also be of great importance in a number of applications. Further, in most of the previous simulation studies, the extracted dynamics is not fully representative of the ions being at the interface. Indeed, the methods used to identify interfacial particles either rely on the separation of the simulation box into layers perpendicular to the axis normal to the liquid surface,[69] or defines the outmost layer through the position of the particles along the macroscopic surface normal axis.[70,71] However, dynamical properties at ionic liquid surfaces are complex and influenced by various factors such as the layer structure of the cation and anion at the interface, the presence of the hydrophobic tails of the ionic liquid, as well as the long-range interactions. This notion further stresses the need for identifying and analyzing the real, capillary wave corrugated intrinsic liquid surface in such studies and, hence, application of intrinsic analysis to analyze the surface dynamics of RTIL is also expected to yield new insight into this problem.

Indeed, both single particle[72-83]and collective dynamics[84,85] of the particles at the intrinsic liquid surface of various atomic[72,73,84,85] and molecular liquids,[74-78,80] as well as liquid mixtures[79,82,83] and salt solutions,[81] have been studied in the past few years. However, we are only aware of a handful of studies of surface dynamics of RTILs where the interface was clearly defined using intrinsic analysis methods. For instance, Lísal et al. used the ITIM algorithm and studied the dynamics of exchange between the liquid surface and the subsequent region, lateral surface diffusion and re-orientational dynamics of the particles at the neat liquid-vapor interface of imidazolium-based RTILs in the absence[45] as well as in the presence[48] of dissolved *n*-hexane molecules. They found a very slow dynamics of the particles as compared to conventional molecular liquids, a slight speed-up of the interfacial dynamics in the presence of hexane, and a correlation between the re-orientational dynamics of the ions and the dynamics of their exchange between the liquid surface and the bulk.[45,48] Palchowdhury and Bhargava studied the surface dynamics in binary mixtures of two ionic

liquids, formed by alkyl-imidazolium cations of different (i.e., C2 and C8) chain lengths with the same trifluoromethansulfonate (TfO^-) anion, employing again the ITIM method. They found that cations with longer chains stay longer at the liquid surface, and their surface residence time increases with decreasing mole fraction. They also suggested that cations with longer alkyl chains retain their orientation with respect to the interface normal for a longer time.[66] Finally, Sedghaniz and Moosavi showed that the residence time of the cations at the interface of a symmetric linear three-cationic RTIL gradually increases with the length of the alkyl chains that link the imidazolium rings.[67]

In this paper, we present a detailed and systematic analysis of the single particle dynamics at the intrinsic liquid surface of a number of imidazolium-based ionic liquids. The systems to be studied are chosen in such a way that the effect of both the size and shape of the anions and the length of the hydrocarbon chain of the cations can be examined. Thus, in the systems studied the 1-butyl-3-methylimidazolium ($bmim^+$) cation is coupled with the BF_4^-, PF_6^-, TfO^-, and bis(trifluoromethylsulfonyl) imide ($NTf2^-$) anions, while, besides $bmim^+$, the PF_6^- anion is also coupled with the 1,3-dimethylimidazolium ($mmim^+$) and 1-octyl-3-methylimidazolium ($omim^+$) cations. Further, we address the effect of temperature by simulating some systems at 298 K and 398 K, and investigate model dependence by repeating the simulation of [bmim][PF_6] with four different potential models. The ions forming the surface layer of the liquid phase as well as those pertaining to the subsequent three subsurface molecular layers are identified by means of the ITIM method.[58] In the analyses, we characterize the dynamics of exchange of the ions between the liquid surface and bulk liquid phase by calculating their survival probability and mean residence time both in the surface layer and in the subsequent layers. To get information on the dynamics of the rotational and torsional motion of the surface ions, the mean residence time of certain representative atoms in the surface atomic layer is also calculated. Finally, the lateral diffusion of the ions at the liquid surface is addressed by calculating their lateral surface diffusion coefficient and the characteristic time of this diffusion, investigating also the relation of this characteristic time with the mean surface residence time of the two ions in the first four molecular layers of the systems simulated.

The remainder of this paper is organized as follows. In sec. 2., details of the calculations, including simulations, ITIM analyses as well as the calculation of the various quantities characterizing the single particle surface dynamics are given. The obtained results are presented and discussed in detail in sec. 3. Finally, in sec. 4, the main conclusions of this study are summarized.

2. Methods

2.1. Molecular Dynamics Simulations

To investigate the single particle dynamics of the individual ions at the liquid-vapor interface of neat imidazolium-based RTILs, we have performed molecular dynamics simulations in the canonical (*N*,*V*,*T*) ensemble. Details of the simulations have been thoroughly described in our previous publication,[53] thus, they are only briefly reminded here.

All systems simulated have consisted of 864 ion pairs in a rectangular basic simulation box. The X edge of the basic box, being perpendicular to the macroscopic plane of the liquid surface, has been twice as long as the Y and Z edges in every case. The lengths of the Y edge, L_Y, of all systems simulated are collected in Table 1. The size of the basic box has been at least an order of magnitude larger in every direction than the Debye screening length of the ions.[53]

The benchmark system in this study is [bmim][PF_6], described by the OPLS-based[86] all-atom model of Doherty et al.,[87] referred to here as the DZGLA model. To investigate the effect of the shape and size of the anions as well as the alkyl chain length of the cations on the surface dynamical properties, we have also performed simulations using the BF_4^-, TfO^-, and $NTf2^-$ anions instead of PF_6^-, and the $mmim^+$ and $omim^+$ cations instead of $bmim^+$. The structure of all the ions considered is illustrated in Figure 1. All systems have been simulated at 298 K, with the exception of [mmim][PF_6], which is still below its melting point at this temperature. Therefore, this system has been simulated at 398 K. Further, to address also the effect of the temperature beside that of the cation chain length, the simulations of [bmim][PF_6] and [omim][PF_6] have been repeated at 398 K. Finally, to address the possible model dependence of the results, we have repeated the [bmim][PF_6] simulation at 298 K with three other potential models, including the original, full-charge version[86] of the DZGLA model, the potential proposed by Bhargava and Balasubramanian[88] as a refinement of the CLaP force field,[89,90] and the united atom model of Zhang et al.[91] These models are referred to here as DZGLA-FC, BB, and ZLC, respectively. It should be noted that all of these models are pairwise additive, all of them except ZLC (which is a united-atom model) use the all-atom approach, and all of them except DZGLA-FC (which is a full-charge model) use a scaled-down nominal ion charge of ±0.8 to account for the polarization of the electron cloud in an average way.[92] Details of the systems simulated are summarized in Table 1.

All simulations have been performed with the GROMACS 2019.3 program package.[93] Equations of motion have been integrated in time steps of 2 fs using the leapfrog algorithm.[94]

To control the temperature of the system, the v-rescale algorithm[95] has been employed. All bond lengths involving a hydrogen atom have been kept fixed using the LINCS method.[96] All interactions have been truncated to zero beyond the group-based cut-off distance of 13.0 Å. The long range part of both the electrostatic and Lennard-Jones interactions has been accounted for by means of the particle mesh Ewald (PME) method in its smooth particle mesh implementation.[97,98]

Initial configurations have been prepared as described in our previous publication.[53] Systems have been equilibrated for at least 0.1 μs. Once equilibrium has been reached, 20000 independent sample configurations have been dumped for the analyses from a subsequent, 0.1 μs long production run. The lengths of these runs turned out to be long enough to provide sufficient equilibration and proper sampling.[53]

2.2. ITIM Analyses

To identify the ions forming the surface layers of the systems studied, the ITIM method[58] has been used. Further, to address the rotational and along-the-surface-normal translational/vibrational motion of the ions, the ITIM analysis has been repeated in atomistic rather than molecular resolution, i.e., by identifying the individual atoms rather than entire ions that are at the liquid surface, as described in our previous publication.[53]

In an ITIM analysis, a spherical probe is moved along test lines parallel with the macroscopic surface normal from the bulk opposite phase towards the liquid surface. Once the probe touches the first particle that belongs to the phase of interest, this particle is marked as being in the surface layer, and the next test line is considered. After the probe is moved along all test lines, the full set of particles that form the interfacial layer (i.e., that are "seen" from the opposite phase by the probe) are identified. Further, by disregarding the particles forming the interfacial layer and repeating the entire procedure, the particles forming the next subsurface layer can also be identified.[58]

ITIM analyses have been performed here by the freely available[99] Pytim software,[100] using, in accordance with previous recommendations,[58,60] a spherical probe with a radius of 2 Å (being the size range of 1.75 -2.5 Å, within which its actual value does not influence the interfacial properties of the systems studied considerably[53]), and a grid of test lines with 0.4 Å spacing in the Y and Z directions. Previously we showed that the results of the ITIM analysis does not depend considerably on the To determine the touching position of the probe sphere with the outmost atom of the liquid phase along a given grid line, the size of the atoms has

been estimated by their Lennard-Jones diameter, σ. Besides the ions forming the surface layer, those belonging to the subsequent three molecular layers have also been determined. The mean number of cations and anions pertaining to the individual layers, $<N_{cat}>$ and $<N_{an}>$, respectively, are included in Table 1. The ions forming the first two subsurface layers for an equilibrium snapshot of the surface portion of the [bmim][PF_6] system, simulated at 298 K with the DZAGLA model, are shown in Figure 2.

2.3. Calculation of the Single Particle Dynamical Properties

2.3.1. Survival Probability at the Surface and Mean Surface Residence Time

The survival probability of a particle at the liquid surface, $L(t)$, is simply the probability that a particle that is part of the surface layer at the time t_0 stays uninterruptedly there until $t_0 + t$. Since the departure of a particle from the liquid surface is a process of first order kinetics, $L(t)$ is an exponentially decaying function, i.e., $L(t) = A\exp(-t/\tau)$, τ being the mean lifetime of the particles at the surface. If the particles can leave the surface by k different mechanisms, $L(t)$ is a sum of k different exponentially decaying functions, i.e.,

$$L(t) = \sum_{i=1}^{k} A_k \exp(-t/\tau_k)\,. \qquad (1)$$

In this equation, A_k and τ_k are the relative weight and characteristic time, respectively, of the k^{th} mechanism. In practice, particles can leave the liquid surface by two different mechanisms, i.e., either due to a fast oscillatory motion – in this case they rapidly return to the surface due to the same oscillation – or permanently, due to their diffusive motion. Thus, the entire duration of the residence of the particles at the liquid surface can be characterized by the τ value of the mechanism of permanent departure, often referred to as the mean surface residence time (denoted here as τ_{res}). It should be noted that the interim departure of the particles from the surface due to their oscillatory movement could also be disregarded through the definition of an intermittent survival probability, i.e., allowing departure from the surface within a pre-defined, short time window, Δt. However, we prefer to distinguish between the two departure mechanisms through a biexponential fit of the $L(t)$ data rather than using an intermittent residence time, as this treatment is not only free from the unavoidably arbitrary choice of Δt, but also better captures the underlying physical phenomena.

2.3.2. Lateral Diffusion Coefficient

The lateral diffusion coefficient of the surface particles in the macroscopic plane of the liquid surface, $D_{\parallel}$, can simply be calculated through the Einstein equation[94] as

$$D_{\parallel} = \frac{MSD}{4t}, \tag{2}$$

(*MSD* being the mean square displacement of the particles in the YZ plane) by fitting a straight line to the calculated *MSD* vs. *t* data. In fact, the *MSD* vs. *t* data follows a linear increase only after an initial period, i.e., when the particles already left the ballistic regime and indeed perform diffusive motion.

The characteristic time of the surface diffusion, τ_D, can be defined as the time during which a diffusing particle explores a surface portion equal to the average area per particle. The value of τ_D can be obtained as[77,101]

$$\tau_D = \frac{L_Y L_Z}{2D_{\parallel} < N_{surf} >}, \tag{3}$$

where L_Y and L_Z are the lengths of the Y and Z edges of the basic box, respectively, and $<N_{surf}>$ is the average number of surface particles.

It should finally be noted that the relation between τ_D and τ_{res} shows whether the particles have enough time to perform noticeable diffusion during their stay at the liquid surface. Thus, if $\tau_{res} >> \tau_D$, the exchange of particles between the liquid surface and the underlying liquid is slow enough to allow the surface particles to explore a considerable portion of the liquid surface by diffusion. Conversely, if $\tau_{res} << \tau_D$, i.e., the surface diffusion occurs on a longer time scale than the mean surface residence time, particles leave the liquid surface without having time to perform noticeable diffusion, and therefore, in this case, surface diffusion cannot be meaningfully discussed.

3. Results and Discussion

3.1. Mean Surface Residence Times of the Ions

To characterize the dynamics of exchange of the ions between the liquid surface and the bulk liquid phase, we have calculated the survival probability, $L(t)$, and mean surface residence time, τ_{res}, of both ions in the first four subsurface molecular layers of the systems simulated, as described in sec. 2.3.1. The obtained $L(t)$ data could always be very well fitted by a biexponential function (eq. 1), as illustrated in Figure 3 on the example of [bmim][NTf2]. The mean residence time values, τ_{res}, obtained from this fit are collected in Table 2, and are shown in Figure 4 separately for the cations (τ_{cat}) and anions (τ_{an}). The characteristic time of the other mechanism, associated with the temporary departure of the ion from the surface layer due to its vibration, τ_{vib}, has indeed turned out to be about at least an order of magnitude smaller than τ_{res} in every case.

As is seen, the surface dynamics of the ions is rather slow. At 298 K, the mean residence time of the cations in the surface layer is in the order of a few nanoseconds, while that of the anions is 2-5 times shorter. Values of a similar order were reported earlier by Lísal et al. using a different potential model.[45,48] For comparison, the typical mean surface residence time of molecular liquids is two orders of magnitude smaller, being around 20 ps for various apolar, aprotic dipolar, and even H-bonding liquids.[77] The increase of the temperature to 398 K leads to considerably, i.e., 5-7 times, shorter surface residence times, as it should be expected. Among the different anions, the exchange of the smaller and more spherical ones between the surface and the bulk phase is clearly faster than that of the larger and more elongated ones. Thus, the mean residence time of the $NTf2^-$ ions in the surface layer is about six times larger than that of BF_4^- (see Table 2). The increase of the length of their alkyl chain slows down the dynamics of exchange of the cations between the surface layer and the bulk, but this effect is weaker than that of the shape and size of the anions, and clearly gets stronger at higher temperature. Thus, the τ_{res} value of the $omim^+$ ions is only 5% larger than that of $bmim^+$ (in the presence of PF_6^- anions) at 298 K, but it is 3 and 1.5 times larger than those of $mmim^+$ and $bmim^+$, respectively, at 398 K.

Considering the change of τ_{res} from layer to layer, it is seen that cations stay about an order of magnitude longer in the surface layer than in the second one, and their mean residence time rapidly decreases from layer to layer upon going farther from the liquid surface (see Table 2 and Fig. 4.a). This behavior marks the gradual loss of the influence of the

vicinity of the vapor phase on the dynamics of the ions. The extremely long residence time of the imidazolium cations at the liquid surface is likely related to the free energy gain achieved by exposing the apolar alkyl groups to the vapor phase.[46,53] This explanation is in line with the aforementioned finding that the increase of the alkyl chain length leads, on average, to a longer stay of the cations at the liquid surface.

The dynamics of exchange of the anions between the surface layer and the bulk liquid phase shows a markedly different behavior. In particular, anions typically stay, on average, somewhat longer in the second than in the first layer, and this difference is larger for smaller anions. Thus, while the τ_{res} value obtained in the second layer is about 90% and 15% larger than that in the first layer for BF_4^- and TfO^-, respectively, these values are almost identical for $NTf2^-$ and PF_6^- (as described by the DZGLA model) at both temperatures considered. Further, the ratio of τ_{res} of the anions in the second and first layers depends sensitively on the alkyl chain length of the cations, i.e., it becomes larger with increasing cationic chain length. Thus, for PF_6^-, this ratio is close to 1 if the cation is $bmim^+$, while it becomes about 0.3 and 2 in the presence of $mmim^+$ and $omim^+$ cations, respectively, regardless of temperature. The origin of this marked effect is twofold: the increase of the cation chain length leads, on average, to a shorter stay of the anions in the first layer, and a longer stay of them in the second layer. The reason for this behavior is likely related to the rather large fractional charges of the anion atoms, which drive them away from the apolar layer of the alkyl chains of the outmost cations.[53] Hence, the larger the surface apolar domains (i.e. the larger the cation chains) are, the more quickly the anions are "pushed" from the surface layer after entering it, and therefore the longer they reside in the subsurface layer.

Our above findings that the increasing size of the anions leads to their longer stay in the first layer, while the increase of the cationic alkyl chain length has clearly an opposite effect, suggest that the *relative* size of the two ions plays an important role in this respect. Thus, in the case of much larger cations than anions (e.g., in [bmim][BF_4] and [omim][PF_6]), cations stay considerably longer at the liquid surface than anions, while both the decrease of the cation chain length and the increase of the size of the anion brings these values closer to each other (see, e.g, [bmim][PF_6] and [bmim][NTf2]). The effect of the relative size of the two ions on their surface dynamics is illustrated in Fig. 4.c, showing the ratio of the τ_{res} values of the cations and anions, τ_{cat}/τ_{an}, in the different subsurface layers of the systems studied. This figure also reveals that although the ratio of the mean surface residence time of the two ions indeed depends on their relative size, this is not the only important factor here. Thus, this

ratio is clearly rather large in the first layer, and typically drops below 1 in the second layer. Both effects get clearly stronger in the case of smaller anions and longer cation alkyl chains. However, both effects nearly cancel out in the case of [mmim][PF_6], for which the τ_{cat}/τ_{an} values fluctuate around unity, i.e., in a system in which the two ions are not only of comparable size, but also the cation completely lacks the apolar alkyl chain. For comparison, this value is about 2.2 and 0.45 in the first and second layer, respectively, of [bmim][NTf2], where the two ions are also of comparable size. In fact, the absence of apolar domains seems to cause a rather pronounced qualitative shift in the ion surface dynamics, since the curve for [mmim][PF_6] is quite different from the rest of the RTIL systems considered. Finally, the increase of the temperature increases the τ_{cat}/τ_{an} ratio in the first layer, presumably because the increasing thermal motion affects the anions more or less isotropically, while the free energy gain of exposing their alkyl chain to the vapor phase still anchors the cations to a large extent to the liquid surface.

It is interesting to note that anions not only stay longer, but also occur more frequently in the second than in the first molecular layer (see Table 1). Similar correlation between the lateral density and mean residence time was found earlier in aqueous alkali halide solutions,[81] and was explained by a simple two-state model for the hopping between the first and the second layer, in accordance with the Kramers theory.[102] From the third layer on, the mean residence time of the anions, similarly to that of the cations, also decreases gradually from layer to layer due to the decreasing influence of the surface on the dynamics of the particles. All these effects are illustrated in Fig. 4.b.

It also turns out that the details of the surface dynamics of the ions are much more sensitive to the details of the potential model chosen than the structural characteristics,[53] probably due to the different distribution of fractional charges among the different atoms (see Tables S1 and S2 of Supporting Material of Ref. 53). Thus, the dynamics of the BB model of [bmim][PF_6] is considerably faster, while, interestingly, that of the united-atom ZLC model is considerably slower than that of the DZGLA model. The latter observation is somewhat counterintuitive, given that coarse-graining into a united-atom description reduces the degrees of freedom and generally tends to speed up the dynamics. Moreover, the use of unscaled ionic charges slows down the dynamics of the particles by about an order of magnitude (compare data for DZGLA and DZGLA-FC in Table 2), in a clear accordance with earlier findings.[103,104] This finding suggests that the ion dynamics is dominated by electrostatics, and that the observed slow dynamics (compared to molecular liquids) is related to the strong electrostatic attraction acting between the oppositely charged ions. Indeed, this attraction,

being a first order (chemical) interaction, is much stronger than the van der Waals, dipolar, or even H-bonding attraction acting between the particles in molecular liquids. It should be noted that ionic systems (even in the case of small and light simple ions) are typically in their solid phase at room temperature, and the unusually low melting point of RTILs is related to the size asymmetry of their ions as well as to the presence of charged and uncharged moieties, rather than to the strength of attraction between the particles.

3.2. Mean Surface Residence Times of Atoms

While the residence times of the entire ions in successive subsurface molecular layers characterize the dynamics of their exchange between the liquid surface and bulk liquid phase, those of individual atoms in the first atomic layer provide information on the dynamics of the out-of-plane rotational and torsional motion of the surface ions. Indeed, while an entire ion departs from the liquid surface due to its diffusion along the surface normal, individual atoms primarily leave the surface because of a vibrational or rotational move of either the entire ion or a part of it. To investigate this point, we have calculated the survival probability and mean surface residence time of the alkyl chain terminal H atoms and ring C atoms of the cations, and of the F atoms of the anions in the surface atomic layer of all systems simulated.

The obtained $L(t)$ data follow biexponential decay rather accurately in every case, as illustrated in Figure 5 for selected systems. The atomistic mean surface residence time values obtained from the biexponential fits, $\tau_{\mathrm{res}}^{\mathrm{at}}$, are collected in Table 3. As is seen, these atomistic $\tau_{\mathrm{res}}^{\mathrm{at}}$ values are two orders of magnitude smaller than those of the entire ions, indicating that individual atoms can rotate away from the intrinsic liquid surface on a much shorter timescale than that corresponding to the departure of the entire ions. Further, they are still about an order of magnitude smaller than the τ_{vib} value of the corresponding ions, confirming that these atoms indeed leave the surface atomic layer due to either a torsional motion or rotation of the ion and not due to its vibration along the surface normal axis. In particular, alkyl terminal H atoms stay typically somewhat longer, while anion F atoms shorter at the liquid surface than ring C atoms. As is expected, at higher temperature not only translation, but also the rotation and internal motions of the ions become faster, as seen from the consistent decrease of the $\tau_{\mathrm{res}}^{\mathrm{at}}$ values with increasing temperature. Surprisingly, the length of the alkyl chain does not have a clear effect on the dynamics of the internal motions and rotations of any of the two ions. On the other hand, the surface residence time of the F atoms is largely influenced by the shape of the anion they belong to. Thus, while in the case of the small and rather spherical

BF_4^- and PF_6^- ions, the τ_{res}^{at} value of the F atoms is about 10 ps, while the τ_{res} value of the F atoms corresponding to the rather elongated $NTf2^-$ and less elongated TfO^- ions is about 7 and 5 times larger, respectively (see also Fig. 5). This suggests that these elongated anions primarily rotate along an axis parallel to the surface normal (which keeps the same atoms at the surface) than along axes perpendicular to the surface normal (which would lead to an exchange of surface atoms). It should finally be noted that the mean surface residence time of the individual atoms, especially those of the cations, shows a similar sensitivity to the choice of the potential model used than that of the entire ions.

3.3. Diffusion at the Liquid Surface

To characterize the lateral mobility of the surface ions, we have calculated their lateral diffusion coefficient within the first four molecular layers beneath the liquid surface, $D_{\|}$, as well as the characteristic time, τ_D, corresponding to this diffusion. Fitting a straight line to the obtained *MSD* vs. *t* data was hindered by two factors. First, due to their very slow dynamics, the ions have been found to stay in the ballistic regime for an unusually long time, on the order of 100 ps. Second, after a few hundred picoseconds, they typically leave the given layer, and hence the *MSD* vs. *t* data become increasingly noisy (or does not even exist beyond a certain time). Nevertheless, with one exception (see Table 2), we have always found a 150-400 ps long time window within which the *MSD* vs. *t* data can be meaningfully fitted by a straight line, and hence the value of the lateral diffusion coefficient can be determined. This fit is illustrated in Figure 6 for the example of [bmim][PF_6] as described by the DZGLA model at 298 K.

The lateral diffusion coefficient values and diffusion characteristic times obtained in the different systems are included in Table 2. The results reveal that surface lateral diffusion is also a very slow process in these systems; furthermore, it remains very slow even upon going away from the liquid surface. Thus, the characteristic time of this diffusion for both ions is typically in the order of a few nanoseconds in every subsurface layer considered, while the value of the lateral diffusion coefficient, $D_{\|}$, typically falls in the range of 1-10 $Å^2$/ns at 298 K. Similar values were obtained by Lísal et al. for [bmim][NTf2] with another potential model.[45,48] Again, in molecular liquids, this value is three orders of magnitude larger, being around 1 $Å^2$/ps.[77] On the other hand, the values obtained here are in the same order than what was previously found in the bulk liquid phase of RTILs both experimentally[105-107] and by computer simulation.[87,88,108] At 398 K, the values of $D_{\|}$ and τ_D are about an order of

magnitude larger and smaller, respectively, than at 298 K. It is also seen that in the first molecular layer, comprising more cations than anions, the diffusion of the anions is typically somewhat faster than that of the cations, while an opposite relation is seen in the second layer, containing an excess amount of anions (see Table 1). This behavior is in clear contrast with that in the bulk, where no meaningful difference was found between the diffusion of cations and anions.[87,88,105-108] This finding suggests that the electrostatic repulsion between like ions that are in excess amount in a given layer slows down their lateral diffusion.

Finally, the comparison of the τ_{res} and τ_D values of the ions (Table 2) reveals that typically only the first layer cations perform noticeable lateral diffusion during their stay in the layer; in all other cases, the ion leaves the layer on a much shorter timescale than that of its lateral diffusion. The reason why cations can diffuse during their stay within the surface layer is clearly that they stay an order of magnitude longer here than other ions in other layers, as discussed in sec. 3.1. The only clear exception in this respect is the case of [mmim][PF_6], in which even the anions stay long enough in the surface layer to perform noticeable diffusion. Further, in [bmim][NTf2$^-$], the characteristic time of the diffusion of the anions in the first layer is comparable with their residence time, indicating that lateral diffusion at the surface occurs on a similar time scale than the dynamics of exchange between the surface and the bulk phase in this case. These findings are illustrated in Figure 7, showing the lateral trajectory of a cation and an anion in the surface layer of selected systems, as taken out from equilibrium trajectories.

4. Conclusions

In this paper, we have analyzed the surface dynamics of imidazolium-based ionic liquids at an unprecedented level of detail. Namely, we systematically examined the effects of cation size, anion type/size, temperature and molecular model on the mean surface residence time and lateral self-diffusion coefficient of both ions, as well as the mean surface residence time of individual atoms pertaining to those ions. Crucially, we applied an intrinsic analysis method (i.e., ITIM), which allowed us to distinguish the dynamical behavior of ions in different individual molecular layers beneath the surface. In this way, we were able to shed light on the subtle balance between electrostatic interactions and polar-apolar segregation on the surface dynamics of RTILs.

It is important to recognize that the models applied in this work lack explicit polarization. While polarizable models are likely to yield a more realistic description of ionic

liquid interfaces,[109] they are also computationally much more intensive. Furthermore, our observations are consistent across several non-polarizable force fields, including those that implicitly account for polarization effects through physically motivated charge scaling.

Our results show that the surface dynamics of the ions is about two to three orders of magnitude slower than that in molecular liquids, with most cations residing for longer at the surface than anions. This slow surface dynamics is mainly caused by strong electrostatic attraction between oppositely charged ions. In particular, lateral diffusion is found to be a generally slower process than the exchange of ions between the subsequent subsurface layers. As a consequence, ions are not able to perform considerable lateral diffusion during their stay in a given subsurface layer. The only marked exception in this respect is the case of the cations in the first layer at the liquid surface due to the roughly one order of magnitude longer residence times of these ions in this layer than those of any other ion in any other layer.

Despite the dominance of electrostatic ion-ion interactions, the presence and size of apolar domains can lead to rather subtle effects on the surface dynamics. For instance, the strong preference of cations to point their apolar chains towards the vapor phase leads to a pronounced increase in their residence time at the first surface layer compared to subsequent layers, with this effect increasing with the size of the alkyl chain. In contrast, anions tend to reside longer in the second layer than at the surface, with this effect being more pronounced for smaller anions, in line with the trend in their lateral density.[53] Interestingly, changes in the cation chain length affect the balance of the anion dynamics, with increasing apolar domains at the surface driving anions into the second molecular layer. Furthermore, there is a clear difference between the diffusion coefficients of anions and cations at the surface – anions diffuse faster in the first layer, while cations diffuse faster in the second layer – in clear contrast to their bulk behavior.

An interesting observation is the rather exceptional nature of [mmim][PF_6] compared to the other ionic liquids analyzed here. For this RTIL, the ratio between cation and anion residence time is close to 1 in every subsurface layer, while it shows a pronounced oscillatory behavior for all the other systems. Furthermore, [mmim][PF_6] is practically the only system in which even the anions stay long enough in the surface layer to perform noticeable diffusion. This suggests that the complete absence of an apolar alkyl chain in the imidazolium cation leads to a rather pronounced qualitative shift in the surface dynamics, with [mmim][PF_6] behaving more like a “conventional” molten salt due to the similar size and shape of its constituent ions. This hypothesis can be further tested by simulating other systems where the ions are both large but have similar shape.

Acknowledgements

This work has been supported by the Hungarian NKFIH Foundation under Project Nos. 149529 and 142256. TUH was supported by the EKÖP-24 University Research Fellowship Program of the Ministry for Culture and Innovation from the source of the National Research, Development and Innovation Fund.

References

(1) Rogers, R. D.; Seddon, K. R. Ionic Liquids - Solvents of the Future? *Science* **2003,** *302*, 792-793.

(2) Wei, P.; Pan, X.; Chen, C. Y.; Li, H. Y.; Yan, X.; Li, C.; Chu, Y. H.; Yan, B. Emerging Impacts of Ionic Liquids on Eco-Environmental Safety and Human Health. *Chem. Soc. Rev.* **2021,** *50*, 13609-13627.

(3) Quintana, A. A.; Sztapka, A. M.; de Carvalho Santos Ebinuma, V.; Agatemor, C. Enabling Sustainable Chemistry with Ionic Liquids and Deep Eutectic Solvents: A Fad or the Future? *Angew. Chem. Int. Ed.* **2022,** 61, e202205609.

(4) Yan, J.; Liu, G.; Chen, H.; Hu, S. ; Wang, X. ; Yan, B. ; Yan, X. ILTox: A Curated Toxicity Database for Machine Learning and Design of Environmentally Friendly Ionic Liquids. *Environ. Sci. Technol. Letters* **2023,** *10*, 983-988.

(5) *Ionic Liquids in Synthesis*; Wasserscheid, P.; Welton, T., Eds.; Wiley-VCH: Weinheim, 2008.

(6) Avila, J.; Corsini, C.; Correa, C. M.; Rosenthal, M.; Pádua, A.; Costa Gomes, M. C. Porous Ionic Liquids Go Green. *ACS Nano* **2023,** *17*, 19508-19513.

(7) Blanchard, L. A.; Hancu, D.; Beckman, E. J.; Brennecke, J. F. Green Processing Using Ionic Liquids and CO_2. *Nature* **1999,** *399*, 28-29.

(8) Anthony, J. L.; Aki, S. N.; Maginn, E. J.; Brennecke, J. F. Feasibility of Using Ionic Liquids for Carbon Dioxide Capture. *Int. J. Environ. Technol. Manage.* **2004,** *4*, 105-115.

(9) Noorani, N.; Mehrdad, A. Solubility of Carbon Dioxide in Some Imidazolium and Pyridinium-Based Ionic Liquids and Correlation with NRTL Model. *Aus. J. Chem.* **2022,** *75*, 353-361.

(10) Zhou, T.; Cui, C.; Sun, L.; Hu, Y.; Lyu, H.; Wang, Z.; Song, Z.; Yu, G. Energy Applications of Ionic Liquids: Recent Developments and Future Prospects. *Chem. Rev.* **2023,** *123*, 12170-12253.

(11) Takács, D.; Katana, B.; Szerlauth, A.; Sebők, D.; Tomšič, M.; Szilagyi, I. Influence of Adsorption of Ionic Liquid Constituents ont he Stability of Layered Double Hydroxide Colloids. *Soft Matter* **2021,** *17*, 9116-9124.

(12) Takács, D.; Varga, G.; Csapo, E.; Jamnik, A.; Tomšič, M.; Szilagyi, I. Delamination of Layered Double Hydroxide in Ionic Liquids under Ambient Conditions. *J. Phys. Chem. Letters* **2022,** *13*, 11850-11856.

(13) Figueiredo, N. M.; Voroshylova, I. V.; Ferreira, E. S. C.; Marques, J. M. C.; Cordeiro, M. N. D. S. Magnetic Ionic Liquids: Current Achievements and Future Perspectives with a Focus on Computational Approaches. *Chem. Rev.* **2024,** *124*, 3392-3415.

(14) Kirchner, B. Ionic Liquids from Theoretical Investigations. In: Ionic Liquids. Topics in Current Chemistry, Vol. 290; Kirchner, B.; Ed.; Springer: Berlin, 2010, pp. 213-262.

(15) Maginn, E. J. Molecular Simulation of Ionic Liquids: Current Status and Future Opportunities. *J. Phys.: Cond. Matter* **2009,** *21*, 373101.

(16) Mondal, A.; Balasubramanian, S. Quantitative Prediction of Physical Properties of Imidazolium Based Room Temperature Ionic Liquids through Determination of Condensed Phase Site Charges: A Refined Force Field. *J. Phys. Chem. B* **2014,** *118*, 3409-3422.

(17) Marekha, B. A.; Koverga, V. A.; Chesneau, E.; Kalugin, O. N.; Takamuku, T.; Jedlovszky, P.; Idrissi, A. Local Structure in Terms of Nearest-Neighbor Approach in 1-Butyl-3-Methylimidazolium-Based Ionic Liquids: MD Simulations. *J. Phys. Chem. B* **2016,** *120*, 5029-5041.

(18) Gehrke, S.; von Domaros, M.; Clark, R.; Hollóczki, O.; Brehm, M.; Welton, T.; Luzar, A.; Kirchner, B. Structure and Lifetimes in Ionic Liquids and their Mixtures. *Faraday Discuss.* **2018,** *206*, 219-245.

(19) Dhakal, P.; Shah, J. K. Recent Advances in Molecular Simulations of Ionic Liquid-Ionic Liquid Mixtures. *Curr. Opin. Green Sustain. Chem.* **2019,** *18*, 90-97.

(20) Kowsari, M. H.; Torabi, S. M. Molecular Dynamics Insights into the Nanoscale Structural Organization and Local Interaction of Aqueous Solutions of Ionic Liquid 1-Butyl-3-methylimidazolium Nitrate. *J. Phys.Chem. B* **2020,** *124*, 6972-6985.

(21) Koverga, V.; Maity, N.; Miannay, F. A.; Kalugin, O. N.; Juhász, Á.; Świątek, A.; Polok, K.; Takamuku, T.; Jedlovszky, P.; Idrissi, A. Voronoi Polyhedra as a Tool for the Characterization of Inhomogeneous Distribution in 1-Butyl-3-Methylimidazolium Cation-Based Ionic Liquids. *J. Phys. Chem. B* **2020,** *124*, 10419-10434.

(22) Chang, T. M.; Billeck, S. E. Structure, Molecular Interactions, and Dynamics of Aqueous [BMIM][BF_4] Mixtures: A Molecular Dynamics Study. *J. Phys. Chem. B* **2021,** *125*, 1227-1240.

(23) Overbeck, V.; Schröder, H.; Bonsa, A. M.; Neymeyr, K.; Ludwig, R. Insights into the Translational and Rotational Dynamics of Cations and Anions in Protic Ionic Liquids by Means of NMR Fast-Field-Cycling Relaxometry. *Phys. Chem. Chem. Phys.* **2021,** *23*, 2663-2675.

(24) Marekha, B. A.; Koverga, V.; Maity, N.; Juhász, Á.; Miannay, F. A.; Inkol, A.; Takamuku, T.; Jedlovszky, P.; Kalugin, O. N.; Idrissi, A. Local Structure in Mixtures of Ionic Liquid with Molecular Solvent: Vibration Spectroscopy, NMR and Molecular Dynamics Simulation. In: *Molecular Basis of Liquids and Liquid-Based Materials*; Nishiyama, K.; Yamaguchi, T.; Takamuku, T.; Yoshida, N., Eds.; Springer Nature: Singapore, 2021, pp. 289-334, and references therein.

(25) Dudariev, D.; Koverga, V.; Kalugin, O.; Miannay, F. A.; Polok, K.; Takamuku, T.; Jedlovszky, P.; Idrissi, A. Insight to the Local Structure of Mixtures of Imidazolium-Based Ionic Liquids and Molecular Solvents from Molecular Dynamics Simulations and Voronoi Analysis. *J. Phys. Chem. B* **2023,** *127*, 2534-2545.

(26) Khudozhitkov, A. E.; Stepanov, A. G.; Kolokolov, D. I.; Ludwig, R. Ion Mobility in Hydroxy-Functionalized Ionic Liquids Depends on Cationic Clustering: Tracking the Alkyl Chain Length Behavior with Deuteron NMR Relaxation. *J. Phys. Chem. B* **2023,** *127*, 9336-9345.

(27) Busch, J.; Kotwica, D.; Al Sheakh, L.; Headen, T.; Youngs, T. G. A.; Paschek, D.; Ludwig, R. Quantification and Distribution of Three Types of Hydrogen Bonds in Mixtures of an Ionic Liquid with the Hydrogen-Bond-Accepting Molecular Solvent DMSO Explored by Neutron Diffraction and Molecular Dynamics Simulations. *J. Phys. Chem. Letters* **2023,** *14*, 2684–2691.

(28) Santos, C. S.; Baldelli, S. Gas-Liquid Interface of Room-Temperature Ionic Liquids. *Chem. Soc. Rev.* **2010,** *39*, 2136-2145, and references therein.

(29) Mezger, M.; Schröder, H., Reichert, H.; Schramm, S.; Okasinski, J. S.; Schröder, S.; Honkimäki, V.; Deutsch, M.; Ocko, B. M.; Ralston, J.; et al. Molecular Layering of

Fluorinated Ionic Liquids at a Charged Sapphire (0001) Surface. *Science* **2008,** *322*, 424-428.

(30) Liu, H.; Liu, Y, Li, J. Ionic Liquids in Surface Electrochemistry. *Phys. Chem. Chem. Phys.* **2010,** *12*, 1685-1697.

(31) Salas, G.; Podgoršek, A.; Campbell, P. S.; Santini, C. C.; Pádua, A. A. H.; Costa Gomes, M. F.; Philippot, K.; Chaudret, B.; Turmine, M. Ruthenium Nanoparticles in Ionic Liquids: Structural and Stability Effects of Polar Solutes. *Phys. Chem. Chem. Phys.* **2011,** *13*, 13527-13536.

(32) Podgoršek, A.; Pensado, A. S.; Santini, C. C.; Costa Gomes, M. F.; Pádua, A. A. H. Interaction Energies of Ionic Liquids with Metallic Nanoparticles: Solvation and Stabilization Effects. J. Phys. Chem. C 2013, 117, 3537-3547.

(33) Fedorov, M. V.; Kornyshev, A. A. Ionic Liquids at Electrified Interfaces. *Chem. Rev.* **2014,** *114*, 2978-3036.

(34) Wang, S.; Li, S.; Cao, Z.; Yan, T. Molecular Dynamic Simulations of Ionic Liquids at Graphite Surface. *J. Phys. Chem. C* **2010,** *114*, 990-995.

(35) Pensado, A. S.; Malberg, F.; Costa Gomes, M. F.; Pádua, A. A. H.; Fernández, J.**;** Kirchner**,** B. Interactions and Structure of Ionic Liquids on Graphene and Carbon Nanotubes Surfaces, *RSC. Adv.* **2014,** *4,* 18017-18024.

(36) Weber, H.; Bredow, T.; Kirchner, B. Adsorption Behavior of the 1,3-Dimethylimidazolium Thiocyanate and Tetracyanoborate Ionic Liquids at Anatase (101) Surface, *J. Phys. Chem. C* **2015,** *119*, 15137-15149.

(37) Weber, H.; Salanne, M.; Kirchner, B. Toward an Accurate Modeling of Ionic Liquid-TiO_2 Interfaces. *J. Phys. Chem. C* **2015,** *119*, 25260-25267.

(38) I. V. Voroshylova, Ers, H.; Koverga, V. Docampo- Álvarez, B.; Pikma, P.; Ivaništšev, V. B.; Cordeiro, M. N. D. S. Ionic Liquid–Metal Interface: The Origins of Capacitance Peaks. *Electrochim. Acta* **2021,** *379*, 138148.

(39) Voegtle, M. J.; Pal, T., Pennathur, A. K.; Menachekanian, S. Patrow, J. G.; Sarkar, S.; Cui, Q.; Dawlaty, J. M. Interfacial Polarization and Ionic Structure at the Ionic Liquid–Metal Interface Studied by Vibrational Spectroscopy and Molecular Dynamics Simulations. *J. Phys. Chem. B* **2021,** *125*, 2741–2753.

(40) Chevrot, G.; Schurhammer, R.; Wipff, G. Molecular Dynamics Simulation of the Aqueous Interface with the [BMI][PF_6] Ionic Liquid: Comparison of Different Solvent Models. *Phys. Chem. Chem. Phys*. **2006,** *8*, 4166-4174.

(41) Bhargava, B. L.; Balasubramanian, S. Layering at an Ionic Liquid−Vapor Interface: A Molecular Dynamics Simulation Study of [bmim][PF6]. *J. Am. Chem. Soc.* **2006,** *128*, 10073–10078.

(42) Lynden-Bell, R. M.; Del Pópolo, M. Simulation of the Surface Structure of Butylmethylimidazolium Ionic Liquids. *Phys. Chem. Chem. Phys*. **2006,** *8*, 949-954.

(43) Sarangi, S. S.; Raju, S. G.; Balasubramanian, S. Molecular Dynamics Simulations of Ionic Liquid–Vapour Interfaces: Effect of Cation Symmetry on Structure at the Interface. *Phys. Chem. Chem. Phys.* **2011,** *13*, 2714–2722.

(44) Hantal, G.; Cordeiro, M. N. D. S.; Jorge, M. What Does an Ionic Liquid Surface Really Look Like? Unprecedented Details from Molecular Simulations. *Phys. Chem. Chem. Phys.* **2011,** *1*3, 21230-21232.

(45) Lísal, M.; Posel, Z.; Izák, P. Air–Liquid Interfaces of Imidazolium-Based [TF_2N^-] Ionic Liquids: Insight from Molecular Dynamics Simulations. *Phys. Chem. Chem. Phys.* **2012,** *14*, 5164-5177.

(46) Hantal, G.; Voroshylova, I.; Cordeiro, M. N. D. S.; Jorge, M. A Systematic Molecular Simulation Study of Ionic Liquid Surfaces Using Intrinsic Analysis Methods. *Phys. Chem. Chem. Phys.* **2012,** *14*, 5200-5213.

(47) Paredes, X.; Fernández, J.; Pádua, A. A. H.; Malfreyt, P.; Malberg, F.; Kirchner, B.; Pensado, A. S. Using Molecular Simulation to Understand the Structure of $[C_2C_1im]^+$–Alkylsulfate Ionic Liquids: Bulk and Liquid–Vapor Interfaces. *J. Phys. Chem. B* **2012,** *116*, 14159–14170.

(48) Lísal, M.; Izák, P. Molecular Dynamics Simulations of n-Hexane at 1-Butyl-3-Methylimidazolium bis(Trifluoromethylsulfonyl) Imide Interface. *J. Chem. Phys.* **2013,** *139*, 014704-1-15.

(49) Paredes, X.; Fernández, J.; Pádua, A. A. H.; Malfreyt, P.; Malberg, F. Kirchner, B.; Pensado, A. S. Bulk and Liquid-Vapor Interface of Pyrrolidinum-Based Ionic Liquids: A Molecular Simulation Study. *J. Phys. Chem. B* **2014,** *118*, 731-742.

(50) Malberg, F.; Hollóczki, O.; Thomas, M. Kirchner, B. En Route Formation of Ion Pairs at the Ionis Liquid-Vacuum Interface. *Struct. Chem.* **2015,** *26*, 1343-1349.

(51) Hantal, G.; Sega, M.; Kantorovich, S.; Schröder, C.; Jorge, M. Intrinsic Structure of the Interface of Partially Miscible Fluids: An Application to Ionic Liquids. *J. Phys. Chem. C.* **2015,** *119*, 28448-28461.

(52) Lapshin, D. N.; Jorge, M.; Campbell, E. E. B.; Sarkisov, L. On Competitive Gas Adsorption and Absorption Phenomena in Thin Films of Ionic Liquids. *J. Mater. Chem. A* **2020,** *8*, 11781-11799.

(53) Tóth Ugyonka, H.; Hantal, G.; Szilágyi, I.; Idrissi, A.; Jorge, M.; Jedlovszky, P. Spatial Organization of the Ions at the Free Surface of Imidazolium-Based Ionic Liquids. *J. Coll. Interface Sci.* **2024,** *676*, 989-1000.

(54) Rowlinson, J. S.; Widom, B. *Molecular Theory of Capillarity*; Dover Publications: Mineola, 2002.

(55) Chacón, E.; Tarazona, P. Intrinsic Profiles Beyond the Capillary Wave Theory: A Monte Carlo Study. *Phys Rev. Letters* **2003,** *91*, 166103.

(56) Chowdhary, J.; Ladanyi, B. M. Water-Hydrocarbon Interfaces: Effect of Hydrocarbon Branching on Interfacial Structure. *J. Phys. Chem. B.* **2006,** *110*, 15442-15453.

(57) Jorge, M.; Cordeiro, M. N. D. S. Intrinsic Structure and Dynamics of the Water/Nitrobenzene Interface. *J. Phys. Chem. C.* **2007,** *111*, 17612-17626.

(58) Pártay, L. B.; Hantal, G.; Jedlovszky, P.; Vincze, Á.; Horvai, G. A New Method for Determining the Interfacial Molecules and Characterizing the Surface Roughness in Computer Simulations. Application to the Liquid–Vapor Interface of Water. *J. Comp. Chem.* **2008,** *29*, 945-956.

(59) Wilard, A. P.; Chandler, D. Instantaneous Liquid Interfaces. *J. Phys. Chem. B.* **2010,** *114*, 1954-1958.

(60) Jorge, M.; Jedlovszky, P.; Cordeiro, M. N. D. S. A Critical Assessment of Methods for the Intrinsic Analysis of Liquid Interfaces. 1. Surface Site Distributions. *J. Phys. Chem. C.* **2010,** *114*, 11169-11179.

(61) Sega, M.; Kantorovich, S.; Jedlovszky, P; Jorge, M. The Generalized Identification of Truly Interfacial Molecules (ITIM) Algorithm for Nonplanar Interfaces. *J. Chem. Phys.* **2013,** *138*, 044110.

(62) Pártay, L. B.; Jedlovszky, P.; Vincze, Á.; Horvai, G. Properties of Free Surface of Water-Methanol Mixtures. Analysis of the Truly Interfacial Molecular Layer in Computer Simulation. *J. Phys. Chem. B.* **2008,** *112*, 5428-5438.

(63) Hantal, G.; Darvas, M.; Pártay, L. B.; Horvai, G.; Jedlovszky, P. Molecular Level Properties of the Free Water Surface and Different Organic Liquid/Water Interfaces, As Seen from ITIM Analysis of Computer Simulation Results. *J. Phys.: Condens. Matter* **2010,** *22*, 284112.

(64) Hantal, G.; Horváth, R. A.; Kolafa, J.; Sega, M.; Jedlovszky, P. Surface Affinity of Alkali and Halide Ions in Their Aqueous Solution: Insight from Intrinsic Density Analysis. *J. Phys. Chem. B* **2020,** *124*, 9884-9897.

(65) Pártay, L. B.; Horvai, G.; Jedlovszky, P. Temperature and Pressure Dependence of the Properties of the Liquid-Liquid Interface. A Computer Simulation and Identification of the Truly Interfacial Molecules Investigation of the Water-Benzene System. *J. Phys. Chem. C* **2010,** *114*, 21681-21693.

(66) Palchowdhury, S.; Bhargava, B. L. Surface Structure and Dynamics of Ions at the Liquid–Vapor Interface of Binary Ionic Liquid Mixtures: Molecular Dynamics Studies. *J. Phys. Chem C* **2016,** *120*, 5430-5441.

(67) Sedghamiz, E.; Moosavi, M. Probing the Tricationic Ionic Liquid/Vacuum Interface: Insights from Molecular Dynamics Simulations. *Phys. Chem. Chem. Phys.* **2018,** *20*, 14251-14263.

(68) Shimada, K.; Kimura, Y. Investigation of Capillary Waves and Thermal Diffusion at the Air–Liquid Interface of Imidazolium-Cation-Based Ionic Liquids Using Transient Grating Spectroscopy. *J. Mol. Liquids* **2023,** *391*, 123269.

(69) Heggen, B.; Zhao, W.; Leroy, F.; Dammers, A. J.; Müller-Plathe, F. Interfacial Properties of an Ionic Liquid by Molecular Dynamics. *J. Phys. Chem, B* **2010,** *114*, 6954-6961.

(70) Yang, D.; Fu, F.; Li, L.; Yang, Z.; Wan, Z.; Hu, N.; Chen, X.; Zeng, G. Unique Orientations and Rotational Dynamics of a 1-Butyl-Imidazolium Hexafluorophosphate Ionic Liquid at the Gas-Liquid Interface: The Effects of the Hydrogen Bond and Hydrophobic Interactions. *Phys. Chem. Chem. Phys.* **2018,** *20*, 12043-12052.

(71) Huang, Q.; Huang, Y.; Luo, Y.; Li, L.; Zhou, G.; Chen, X.; Yang, Z. Molecular-Level Insights into the Structures, Dynamics, and Hydrogen Bonds of the Ethylammonium Nitrate Protic Ionic Liquid at the Liquid-Vacuum Interface. *Phys. Chem. Chem. Phys.* **2020,** *22*, 13780-13789.

(72) Delgado-Buscalioni, R.; Chacón, E.; Tarazona, P. Hydrodynamics of Nanoscopic Capillary Waves. *Phys. Rev. Letters* **2008,** *101*, 106102-1-4.

(73) Duque, D.; Tarazona, P.; Chacón, E. Diffusion at the Liquid-Vapor Interface. *J. Chem. Phys.* **2008,** *128*, 134704-1-10.

(74) Benjamin, I. Solute Orientational Dynamics at the Water/Carbon Tetrachloride Interface. *J. Phys. Chem. C* **2008,** *112*, 8969-8975.

(75) Benjamin, I. Reactivity and Dynamics at Liquid Interfaces. In: *Reviews in Computational Chemistry*, Parrill, A. L.; Lipkowitz, K. B., Eds.; Wiley: Chichester, 2015; Vol. 28, pp. 205-313.

(76) Fábián, B.; Senćanski, M. V.; Cvijetić, I. N.; Jedlovszky, P.; Horvai, G. Dynamics of the Water Molecules at the Intrinsic Liquid Surface As Seen from Molecular Dynamics Simulation and Identification of Truly Interfacial Molecules Analysis. *J. Phys. Chem. C* **2016,** *120*, 8578-8588.

(77) Fábián, B.; Horvai, G.; Sega, M.; Jedlovszky, P. Single Particle Dynamics at the Intrinsic Surface of Various Apolar, Aprotic Dipolar, and Hydrogen Bonding Liquids As Seen from Computer Simulations. *J. Phys. Chem. B* **2017,** *121*, 5582-5594.

(78) Karnes, J. J.; Benjamin, I. Miscibility at the Immiscible Liquid/Liquid Interface: A Molecular Dynamics Study of Thermodynamics and Mechanism. *J. Chem. Phys.* **2018,** *148*, 034707-1-10.

(79) Horváth, R. A.; Fábián, B.; Szőri, M.; Jedlovszky, P. Investigation of the Liquid-Vapour Interface of Aqueous Methylamine Solutions by Computer Simulation Methods. *J. Mol. Liquids* **2019,** *288*, 110978.

(80) Fábián, B.; Horvai, G.; Sega, M.; Jedlovszky, P. Single Particle Dynamics at the Liquid-Liquid Interface. Molecular Dynamics Simulation Study of the Water-CCl_4 System. *J. Phys. Chem. C* **2020,** *124*, 2039-2049.

(81) Hantal, G.; Kolafa, J.; Sega, M.; Jedlovszky, P. Single Particle Dynamics at the Intrinsic Surface of Aqueous Alkali Halide Solutions, *J. Phys. Chem. B* **2021,** *125*, 665-679.

(81) Fábián, B.; Horvai, G.; Idrissi, A.; Jedlovszky, P. Structure and Single Particle Dynamics of the Vapour-Liquid Interface of Acetone-CO_2 Mixtures. *J. Mol. Liquids* **2021,** *334*, 116091.

(83) Honti, B.; Fábián, B.; Idrissi, A.; Jedlovszky, P. Surface Properties of *N*,*N*-Dimethylformamide−Water Mixtures, As Seen from Computer Simulations. *J. Phys. Chem. B* **2023,** *127*, 1050-1062.

(84) Malgaretti, P.; Bafile, U.; Vallauri, R.; Jedlovszky, P.; Sega, M. Surface Viscosity in Simple Liquids. *J. Chem. Phys.* **2023,** *158*, 114705.

(85) Jedlovszky, P.; Sega, M. Surface Viscosity of Liquid Interfaces from Green-Kubo Relations. *J. Chem. Phys.* **2024,** *160*, 201101.

(86) Sambasivarao, S.V.; Acevedo, O. Development of OPLS-AA Force Field Parameters for 68 Unique Ionic Liquids, *J. Chem. Theory Comput.* **2009,** *5*, 1038-1050.

(87) Doherty, B.; Zhong, X.; Gathiaka, S.; Li, B.; Acevedo, O. Revisiting OPLS Force Field Parameters for Ionic Liquid Simulations. *J. Chem. Theory Comput.* **2017,** *13*, 6131-6145.

(88) Bhargava, B. L.; Balasubramanian, S. Refined Potential Model for Atomistic Simulations of Ionic Liquid [bmim][PF_6]. *J. Chem. Phys.* **2007,** *127*, 114510.

(89) Canongia Lopes, J. N.; Deschamps, J.; Pádua, A. A. H. Modeling Ionic Liquids Using a Systematic All-Atom Force Field, *J. Phys. Chem. B* **2004,** *108*, 2038-2047.

(90) Canongia Lopes, J. N.; Deschamps, J.; Pádua, A. A. H. Modeling Ionic Liquids Using a Systematic All-Atom Force Field (Addition and Correction), *J. Phys. Chem. B* **2004,** *108*, 11250-11250.

(91) Zhong, X.; Liu, Z.; Cao, D. Improved Classical United-Atom Force Field for Imidazolium-Based Ionic Liquids: Tetrafluoroborate, Hexafluorophosphate, Methylsulfate, Trifluoromethylsulfonate, Acetate, Trifluoroacetate, and Bis(trifluoromethylsulfonyl)amide. *J. Phys. Chem. B* **2011,** *115*, 10027-10040.

(92) Jorge, M. Theoretically-Grounded Approaches to Account for Polarization Effects in Fixed-Charge Force Fields. *J. Chem. Phys.* **2024,** *161*, 180901.

(93) Abraham, M. J.; Murtola, T.; Schulz, R.; Páll, S.; Smith, J. C.; Hess, B.; Lindahl, E. GROMACS: High Performance Molecular Simulations Through Multi-Level Parallelism from Laptops to Supercomputers. *SoftwareX* **2015,** *1-2*, 19-25.

(94) Allen, M. P.; Tildesley, D. J. *Computer Simulation of Liquids*; Clarendon: Oxford, 1987.

(95) Bussi, G.; Donadio, D.; Parrinello, M. Canonical Sampling through Velocity Rescaling. *J. Chem. Phys.* **2007,** *126*, 014101.

(96) Hess, B. P-LINCS: A Parallel Linear Constraint Solver for Molecular Simulation. *J. Chem. Theory Comput.* **2008,** *4*, 116-122.

(97) Essman, U.; Perera, L.; Berkowitz, M. L.; Darden, T.; Lee, H.; Pedersen, L. G. A Smooth Particle Mesh Ewald Method. *J. Chem. Phys.* **1995,** *103*, 8577-8594.

(98) in't Veld, P. J.; Ismail, A. E.; Grest, G. S. Application of Ewald Summations to Long–Range Dispersion Forces. *J. Chem. Phys*. **2007,** *127*, 144711-1-8.

(99) URL: https://github.com/Marcello-Sega/pytim (last accessed: October 18, 2024).

(100) Sega, M.; Hantal, G.; Fábián, B.; Jedlovszky, P. Pytim: A Python Package for the Interfacial Analysis of Molecular Simulations. *J. Comp. Chem.*, **2018,** *39*, 2118-2125.

(101) Rideg, N. A.; Darvas, M.; Varga, I.; Jedlovszky, P. Lateral Dynamics of Surfactants at the Free Water Surface. A Computer Simulation Study. *Langmuir* **2012,** *28*, 14944-14953.

(102) Hänggi, P.; Talkner, P.; Borkovec, M. Reaction-Rate Theory: Fifty Years After Kramers. *Rev. Mod. Phys.* **1990,** *62*, 251-341.

(103) Liu, Z.; Huang, S.; Wang, W. A Refined Force Field for Molecular Simulation of Imidazolium-Based Ionic Liquids. *J. Phys. Chem. B* **2004,** *108*, 12978–12989.

(104) Schröder, C. Comparing Reduced Partial Charge Models with Polarizable Simulations of Ionic Liquids. *Phys. Chem. Chem. Phys.* **2012,** *14*, 3089-3102.

(105) Tokuda, H.; Hayamizu, K.; Ishii, K.; Susan, A. B. H.; Watanabe, M. Physicochemical Properties and Structures of Room Temperature Ionic Liquids. 1. Variation of Anionic Species. *J. Phys. Chem. B* **2004,** *108*, 16593-16600.

(106) Tokuda, H.; Tsuzuki, S.; Susan, M. A. B. H.; Hayamizu, K.; Watanabe, M. How Ionic Are Room-Temperature Ionic Liquids? An Indicator of the Physicochemical Properties. *J. Phys. Chem. B* **2006,** *110*, 19593−19600.

(107) Marekha, B. A.; Kalugin, O. N.; Bria, M.; Buchner, R.; Idrissi, A. Translational Diffusion in Mixtures of Imidazolium ILs with Polar Aprotic Molecular Solvents. *J. Phys. Chem. B* **2014,** *118*, 5509-5517.

(108) Mondal, A.; Balasubramanian, S. Quantitative Prediction of Physical Properties of Imidazolium Based Room Temperature Ionic Liquids through Determination of Condensed Phase Site Charges: A Refined Force Field. *J. Phys. Chem. B* **2014,** *118*, 3409-3422.

(109) Bedrov, D.; Piquemal, J. P.; Borodin, O.; MacKerell Jr., A. D.; Roux, B.; Schröder, C. Molecular Dynamics Simulations of Ionic Liquids and Electrolytes Using Polarizable Force Fields. *Chem. Rev.* **2019,** *119*, 7940-7995.

Tables

Table 1. Characteristics of the Systems Simulated.

cation	anion	model	T/K	layer	L_Y/Å	$\langle N_{cat} \rangle$	$\langle N_{an} \rangle$
$bmim^+$	BF_4^-	DZGLA	298	1	66.2563	195.4	79.0
				2		112.8	205.8
				3		157.3	136.3
				4		151.8	152.4
$bmim^+$	TfO^-	DZGLA	298	1	68.0538	198.3	115.5
				2		108.7	186.5
				3		155.5	126.3
				4		142.3	149.2
$bmim^+$	$NTf2^-$	DZGLA	298	1	73.2523	185.9	140.7
				2		116.8	167.3
				3		148.7	138.5
				4		146.1	143.0
$bmim^+$	PF_6	DZGLA	298	1	67.2712	184.3	94.2
				2		109.0	188.0
				3		150.8	130.8
				4		144.7	144.2
$omim^+$	PF_6	DZGLA	298	1	74.0365	238.5	43.3
				2		78.9	263.5
				3		172.5	128.2
				4		163.1	155.0
$mmim^+$	PF_6	DZGLA	398	1	62.1378	141.9	125.8
				2		124.8	139.3
				3		136.7	125.5
				4		130.8	133.4
$bmim^+$	PF_6	DZGLA	398	1	67.2712	171.0	102.8
				2		121.6	171.1
				3		146.2	135.3
				4		143.3	143.0
$omim^+$	PF_6	DZGLA	398	1	74.0365	218.9	57.2
				2		100.7	242.6
				3		168.4	138.3
				4		163.0	155.6
$bmim^+$	PF_6	DZGLA-FC	298	1	67.2712	195.0	88.4
				2		104.2	198.6
				3		155.7	131.6
				4		143.9	147.6
$bmim^+$	PF_6	BB	298	1	67.2712	191.0	63.8
				2		83.7	200.0
				3		146.8	123.3
				4		138.7	138.6
$bmim^+$	PF_6	ZLC	298	1	67.2712	204.8	91.4
				2		92.1	199.8
				3		155.3	126.4
				4		142.3	147.2

Table 2. Dynamical Properties of the Cations and Anions in Their First Four Molecular Layers at the Liquid Surface. Time Values Set by Bold Mark the Cases Where Ions Exhibit Noticeable Lateral Diffusion during Their Stay in the Layer.

salt	model	T/K	layer	cation			anion		
				τ_{res}/ns	τ_D/ns	$D_\parallel$/Å^{2}ns^{-1}	τ_{res}/ns	τ_D/ns	$D_\parallel$/Å^{2}ns^{-1}
[bmim][BF_4]	DZGLA	298	1	**2.35**	**1.2**	6.8	0.219	0.54	15
			2	0.192	0.78	8.9	0.410	1.7	4.2
			3	0.104	1.5	4.9	0.172	1.4	5.4
			4	0.054	1.3	5.4	0.077	2.3	3.2
[bmim][TfO]	DZGLA	298	1	**3.11**	**1.9**	**3.9**	0.863	2.5	3.0
			2	0.508	1.4	5.5	0.976	2.5	3.1
			3	0.377	1.4	6.0	0.388	2.7	3.1
			4	0.156	1.7	4.7	0.173	1.8	4.3
[bmim][NTf2]	DZGLA	298	1	**2.87**	**1.8**	**4.4**	**1.30**	**1.3**	**6.4**
			2	0.575	1.9	4.9	1.26	1.4	6.9
			3	0.491	2.6	3.6	0.441	1.1	8.3
			4	0.250	1.2	8.0	0.372	0.9	10
[bmim][PF_6]	DZGLA	298	1	**3.45**	**2.1**	**3.9**	0.768	1.9	4.4
			2	0.460	1.8	4.3	0.771	2.3	3.3
			3	0.356	3.7	2.2	0.218	5.1	1.6
			4	0.246	1.5	5.1	0.257	3.1	2.5
[omim][PF_6]	DZGLA	298	1	**3.69**	**1.8**	**5.5**	0.616	0.76	13
			2	0.410	8.4	1.0	1.26	7.2	1.1
			3	0.298	8.3	1.1	0.235	16	0.60
			4	0.193	2.1	4.1	0.220	5.7	1.5
[mmim][PF_6]	DZGLA	398	1	**0.278**	**0.18**	**39**	**0.307**	**0.21**	**34**
			2	0.064	0.31	24	0.093	0.34	22
			3	0.053	0.32	23	0.049	0.60	12
			4	0.041	0.20	37	0.043	0.48	15
[bmim][PF_6]	DZGLA	398	1	**0.547**	**0.27**	**30**	0.113	0.18	47
			2	0.062	0.25	30	0.108	0.34	23
			3	0.047	0.18	46	0.052	0.30	27
			4	0.035	0.34	23	0.041	0.32	25
[omim][PF_6]	DZGLA	398	1	**0.827**	**0.60**	**17**	0.084	0.28	36
			2	0.064	0.14	56	0.154	0.59	13
			3	0.060	0.21	42	0.056	0.69	13
			4	0.046	0.26	33	0.052	0.37	23
[bmim][PF_6]	DZGLA-FC	298	1	**22.0**	**10**	**0.79**	1.68	2.0	4.0
			2	1.81	6.4	1.2	2.99	11	0.67
			3	1.37	10	0.78	1.11	6.2	1.3
			4	0.634	13	0.62	0.864	5.1	1.5
[bmim][PF_6]	BB	298	1	**1.96**	**1.5**	**5.9**	0.158	1.1	8.0
			2	0.143	-[a]	-[a]	0.368	3.1	2.5
			3	0.142	24	0.35	0.101	0.55	15
			4	0.085	1.3	6.1	0.094	2.4	3.4
[bmim][PF_6]	ZLC	298	1	**9.27**	**4.0**	**1.9**	1.18	4.7	1.6
			2	0.643	3.7	2.0	1.56	5.7	1.3
			3	0.407	2.1	3.7	0.237	1.6	4.8
			4	0.156	7.3	1.0	0.191	3.5	2.1

[a] *MSD* vs. *t* data could not be fitted by a straight line in any reasonably wide time window.

Table 3. Mean Residence Time of Certain Atoms of the Cations and Anions in the Surface Atomic Layer of the Systems Simulated. For Reference, the Mean Surface Residence Time of the Entire Ions in the Surface Molecular Layer Is also Given. All Time Values Are in ps Units.

salt	model	*T*/K	cations				anions		
			alkyl terminal H atoms	ring C atoms	entire ion		F atoms	entire ion	
					τ_{vib}	τ_{res}		τ_{vib}	τ_{res}
[bmim][BF_4]	DZGLA	298	33.0	28.1	174	2350	11.2	23	219
[bmim][TfO]	DZGLA	298	39.7	30.0	110	3110	51.1	76	863
[bmim][NTf2]	DZGLA	298	58.0	31.2	202	2870	73.6	86	1300
[bmim][PF_6]	DZGLA	298	55.7	33.3	81	3450	9.2	58	768
[omim][PF_6]	DZGLA	298	27.5	21.0	250	3690	9.6	42	616
[mmim][PF_6]	DZGLA	398	10.8	20.5	22	278	10.5	26	307
[bmim][PF_6]	DZGLA	398	21.0	9.5	40	547	8.4	15	113
[omim][PF_6]	DZGLA	398	18.7	12.0	96	827	7.8	11	84
[bmim][PF_6]	DZGLA-FC	298	88.9	135	203	22000	9.2	63	1680
[bmim][PF_6]	BB	298	37.4	17.7	123	1960	7.6	17	158
[bmim][PF_6]	ZLC	298	-[a]	46.5	300	9270	3.8	60	1180

[a]This is a united-atom model, hence has no terminal H atoms.

Figure legends

Figure 1. Structure of the ions considered in this study. B, P, S, N, C, O, F, and H atoms are shown by green, orange, yellow, blue, grey, red, purple, and white balls, respectively.

Figure 2. Equilibrium snapshot of the surface portion of the [bmim][PF_6] system, simulated at 298 K with the DZGLA model. Cations and anions pertaining to the first molecular layer are shown by blue and red colors, respectively, those pertaining to the second layer by green and orange colors, respectively, while ions staying beneath the second layer are represented by thin grey sticks.

Figure 3. Survival probability of the cations (top) and anions (bottom) in the first (black symbols), second (red symbols), third (green symbols), and fourth (blue symbols) molecular layer beneath the liquid surface in [bmim][NTf2], together with their biexponential fit (lines). The inset shows the same data for the cations (filled symbols) and anions (open symbols) of the first layer, along with their biexponential fits (lines) on a logarithmic scale.

Figure 4. Mean surface residence time of (a) the cations and (b) the anions, as well as (c) the ratio of these values, as obtained in the first four molecular layers of the systems simulated. Top panels: systems consisting of $bmim^+$ cations and BF_4^- (red squares), PF_6^- (black circles), TfO^- (green diamonds), and $NTf2^-$ (blue up triangles) anions, simulated at 298 K with the DZGLA model. Middle panels: systems consisting of PF_6^- anions and $mmim^+$ (grey squares), $bmim^+$ (black circles), and $omim^+$ (brown down triangles) cations, simulated at 298 K (full symbols) and 398 K (open symbols) with the DZGLA model. Bottom panels: [bmim][PF_6], simulated at 298 K with the DZGLA (black), DZGLA-FC (purple), BB (magenta), and ZLC (orange) models. The lines connecting the points are just guides to the eye.

Figure 5. Survival probability of the H atoms of the butyl chain terminal CH_3 group (filled black triangles), C atoms of the imidazolium ring (filled red squares), and F atoms of the anions (open blue circles) in the first atomic layer of the [bmim][PF_6] (top panel), [bmim][TfO] (middle panel), and [bmim][NTf2] (bottom panel) systems, described with the DZGLA model, at 298 K. The biexponential fits of the obtained data are also shown (solid curves of respective colors). The inset shows the same data for [bmim][PF_6] on a logarithmic scale.

Figure 6. Linear portion of the *MSD* vs. *t* data of the cations (top) and anions (bottom), as obtained in the first (black symbols), second (red symbols), third (green symbols), and fourth (blue symbols) molecular layer beneath the liquid surface of [bmim][PF_6], described by the DZGLA model at 298 K, along with their linear fits (lines).

Figure 7. Trajectory of a cation and an anion in the macroscopic plane of the liquid surface, *YZ*, during their residence at the liquid surface, as taken from the equilibrated simulations of [bmim][BF_4] (brown and green lines, respectively), [bmim][NTf2] (purple and black lines, respectively), [mmim][PF_6] (blue and red lines, respectively), as well as [bmim][PF_6], simulated with the DZGLA model at 298 K (orange and khaki lines, respectively) and at 398 K (magenta and grey lines, respectively). The ratio of τ_{res} and τ_D is also indicated. The surface residence times of the chosen ions are close to their mean value in every case.

Figure 1.

Tóth Ugyonka et al.

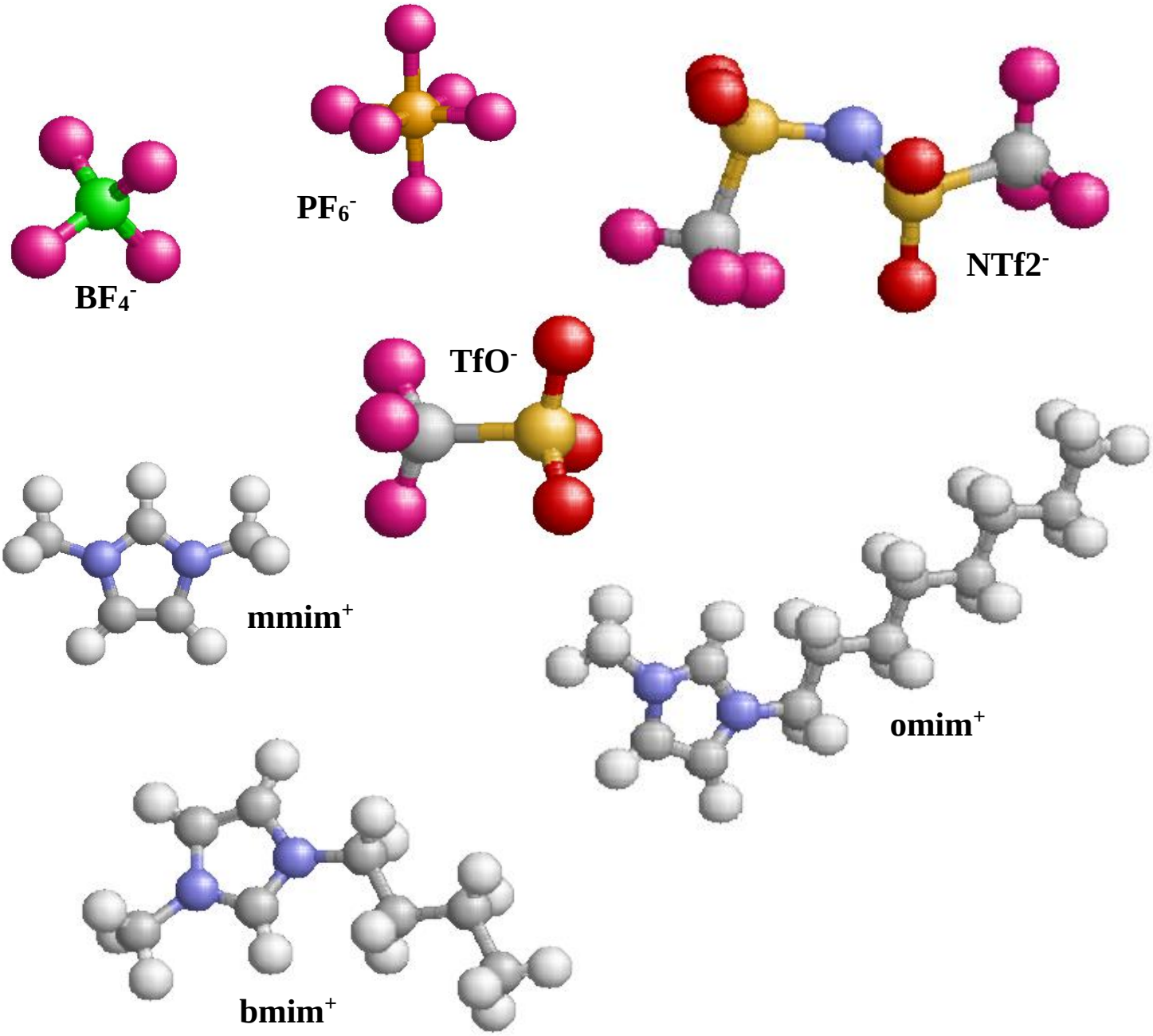

Figure 2.

Tóth Ugyonka et al.

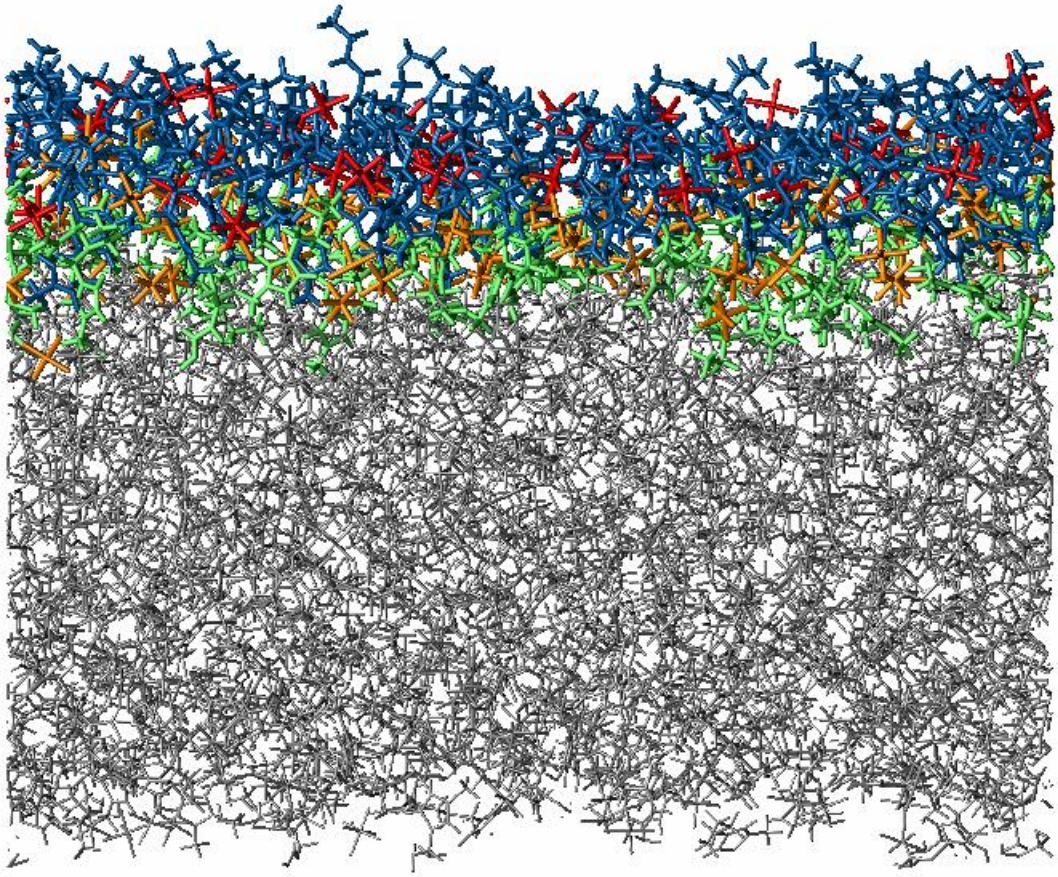

Figure 3.

Tóth Ugyonka et al.

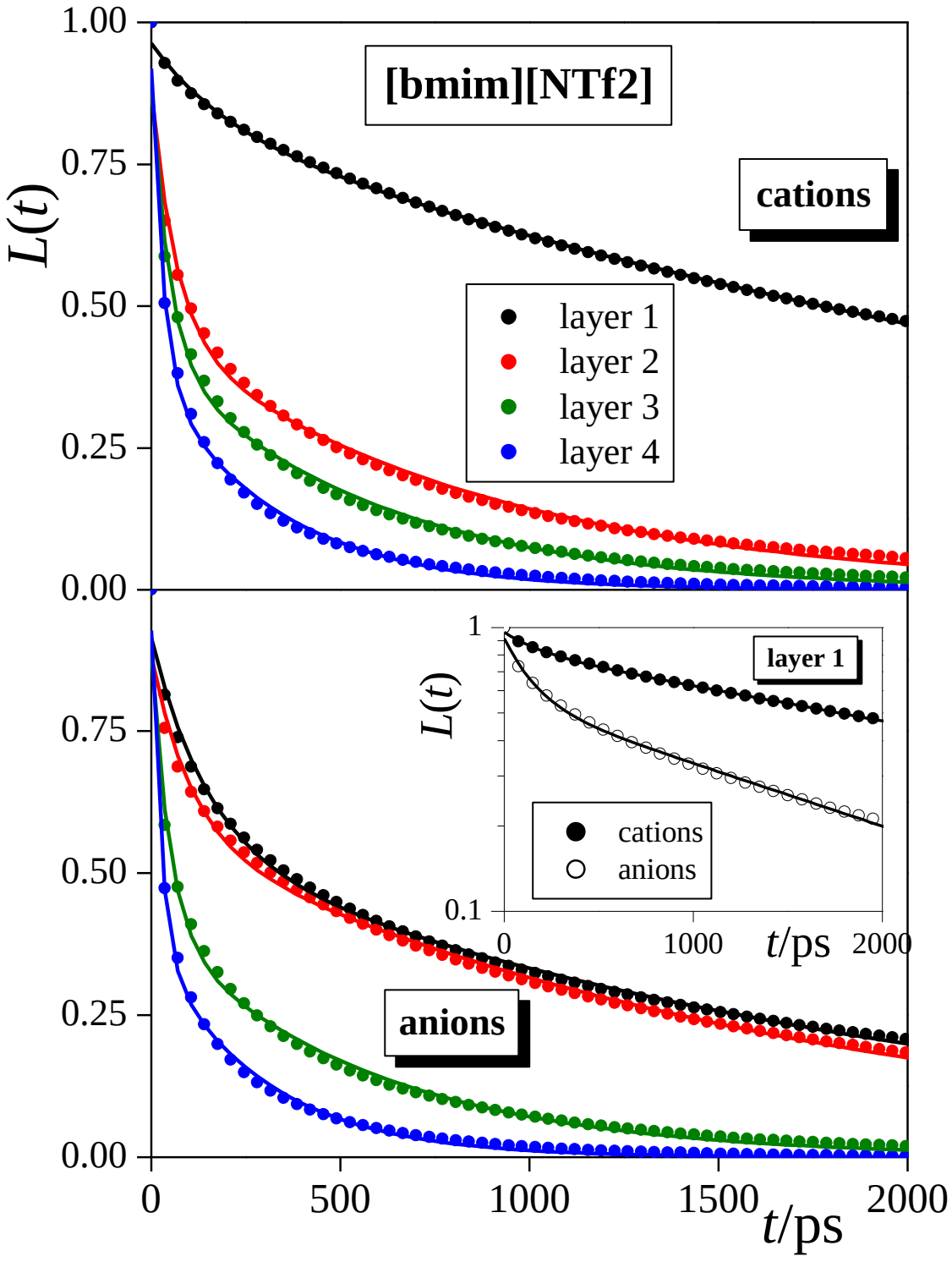

Figure 4.

Tóth Ugyonka et al.

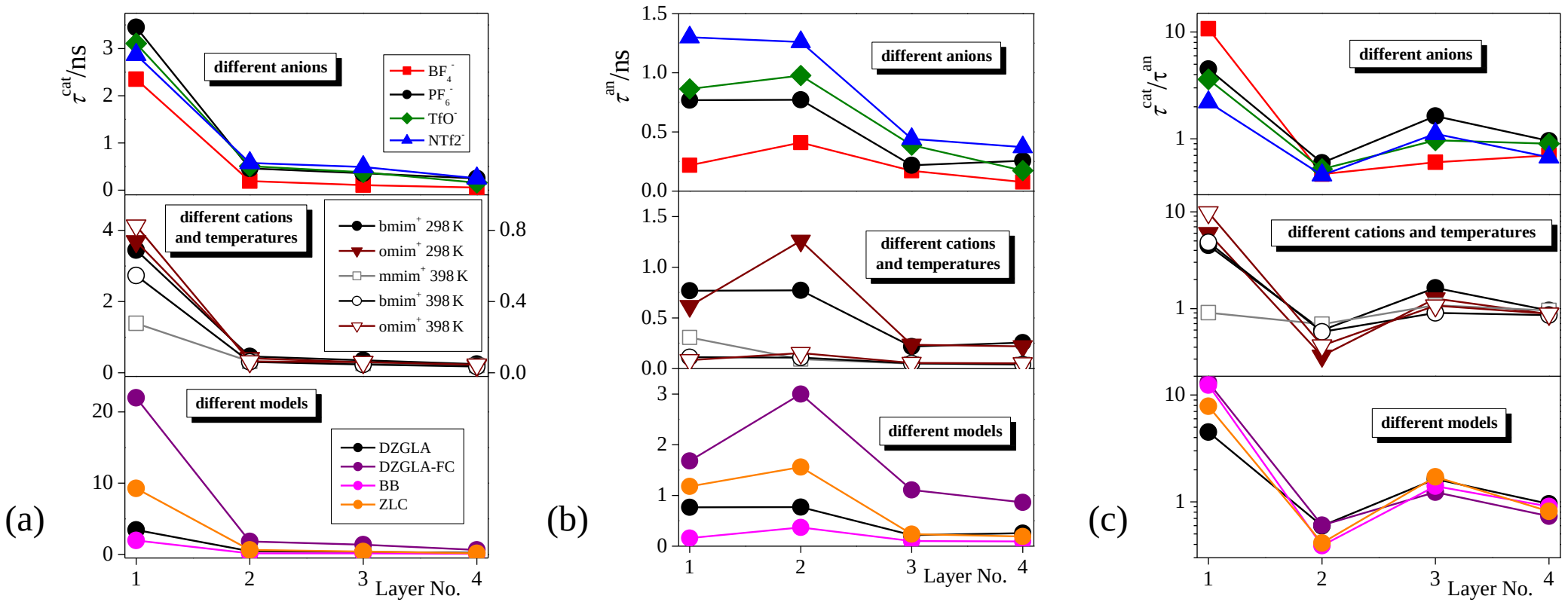

Figure 5.

Tóth Ugyonka et al.

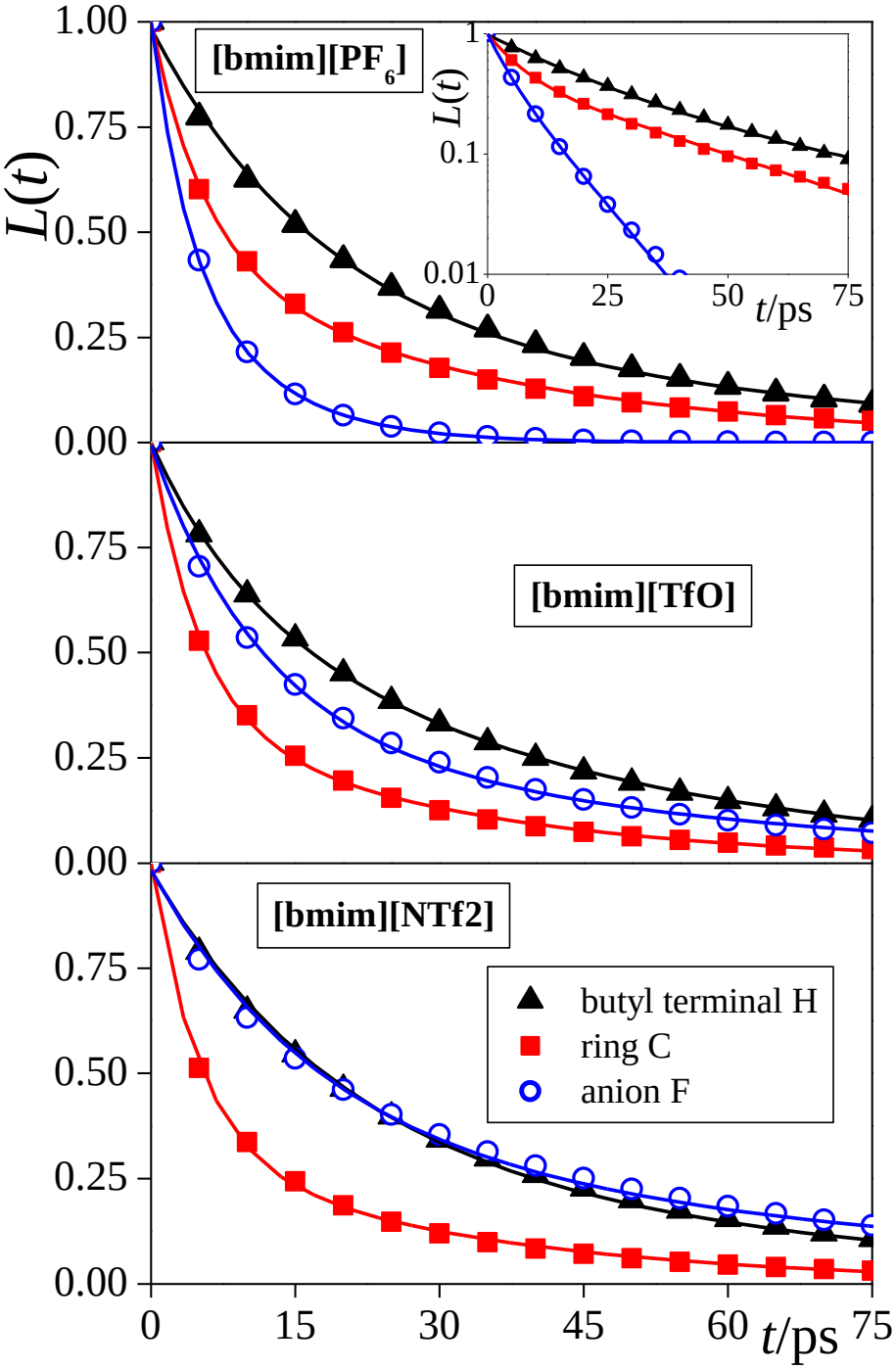

Figure 6.

Tóth Ugyonka et al.

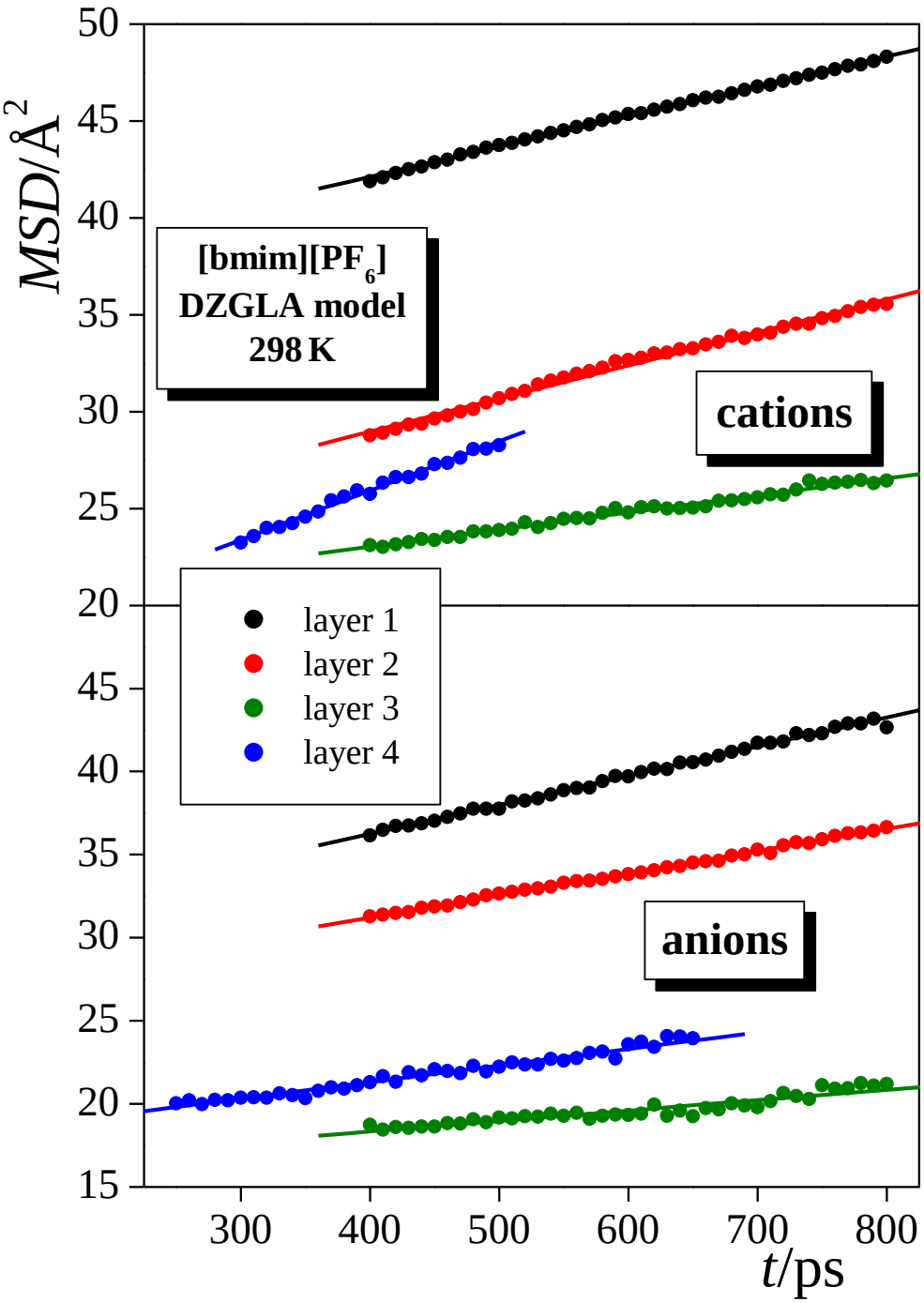

Figure 7.

Tóth Ugyonka et al.

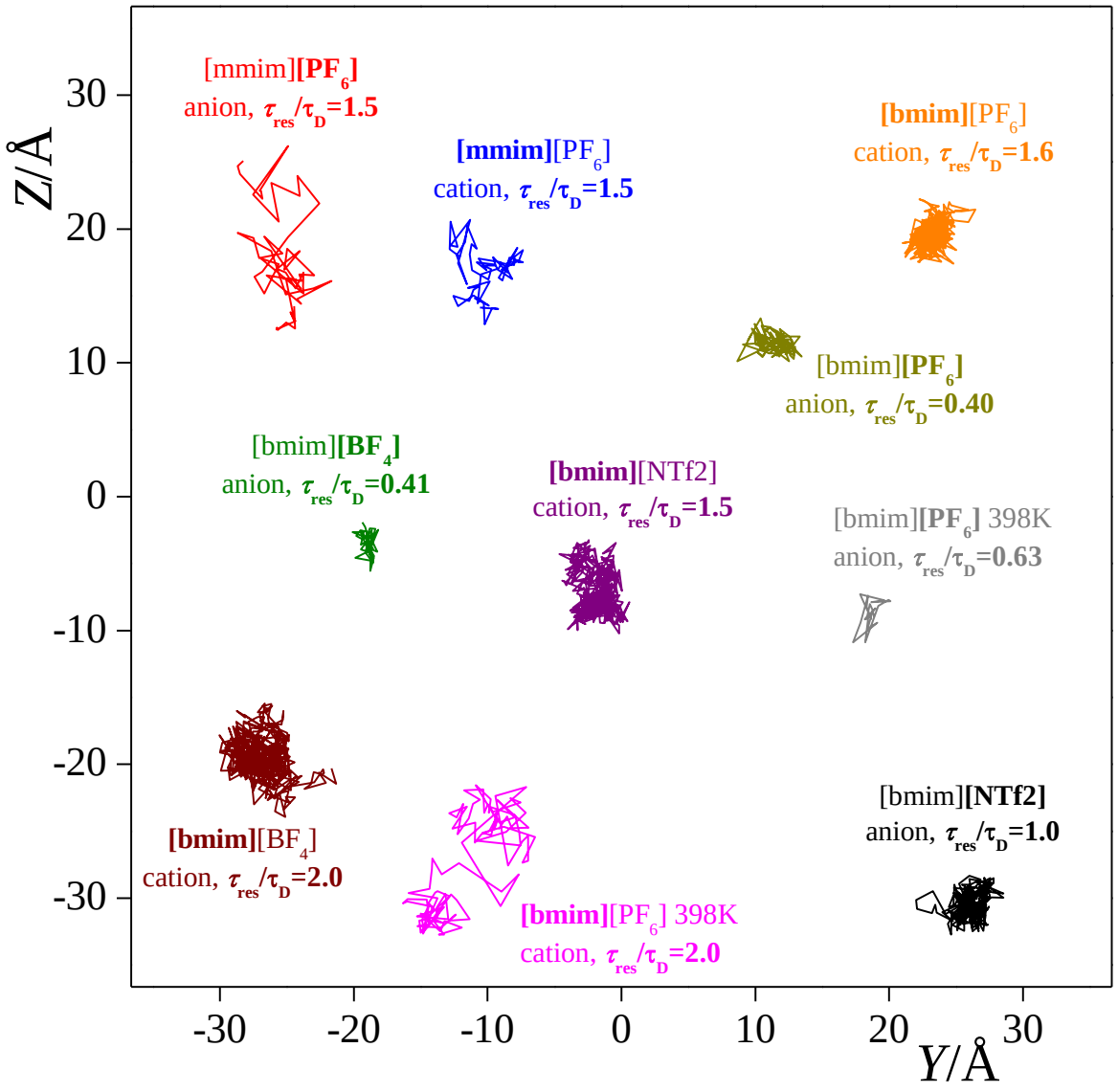

Single particle dynamics at the free surface of imidazolium-based ionic liquids

TOC Graphic: